Alum adjuvant boosts adaptive immunity by inducing uric acid and activating inflammatory dendritic cells

Mirjam Kool,[1] Thomas Soullié,[1] Menno van Nimwegen,[1] Monique A.M. Willart,[1,2] Femke Muskens,[1] Steffen Jung,[3] Henk C. Hoogsteden,[1] Hamida Hammad,[1,2] and Bart N. Lambrecht[1,2]

[1]Department of Pulmonary Medicine, Erasmus University Medical Centre, 3015 GD Rotterdam, Netherlands
[2]Laboratory of Immunoregulation, University Hospital Ghent, 9000 Ghent, Belgium
[3]Weizmann Institute, Rehovot 76100, Israel

Alum (aluminum hydroxide) is the most widely used adjuvant in human vaccines, but the mechanism of its adjuvanticity remains unknown. In vitro studies showed no stimulatory effects on dendritic cells (DCs). In the absence of adjuvant, Ag was taken up by lymph node (LN)–resident DCs that acquired soluble Ag via afferent lymphatics, whereas after injection of alum, Ag was taken up, processed, and presented by inflammatory monocytes that migrated from the peritoneum, thus becoming inflammatory DCs that induced a persistent Th2 response. The enhancing effects of alum on both cellular and humoral immunity were completely abolished when CD11c$^+$ monocytes and DCs were conditionally depleted during immunization. Mechanistically, DC-driven responses were abolished in MyD88-deficient mice and after uricase treatment, implying the induction of uric acid. These findings suggest that alum adjuvant is immunogenic by exploiting "nature's adjuvant," the inflammatory DC through induction of the endogenous danger signal uric acid.

CORRESPONDENCE
Bart N. Lambrecht:
bart.lambrecht@ugent.be

Abbreviations used: Ag, antigen; Alum, aluminum hydroxide; CLN, cervical LN; DLN, draining LN; DT, diphteria toxin; DTR, DT receptor; ILN, inguinal LN; i.t., intratracheal; MLN, mediastinal LN; Tg, transgenic.

Aluminum-containing adjuvants have historically served as immunopotentiators in vaccines and continue to be the most widely used clinical adjuvants (1). Despite the fact that millions of doses of aluminum-containing adjuvants have been given to healthy populations, it is surprising that there is no consensus regarding the mechanisms by which they potentiate the immune system (2–7). The following three potential mechanisms are frequently cited to explain how these adjuvants increase humoral immunity, although scarce experimental evidence is publicly available: (a) the formation of a depot by which the Ag is slowly released to enhance the antibody production; (b) the induction of inflammation, thus recruiting and activating APCs that capture the Ag (8); and (c) the conversion of soluble Ag into a particulate form so that it is phagocytosed by APCs such as macrophages, DCs, and B cells. It is common knowledge that aluminum-containing adjuvants (alum) predominantly induce humoral immunity, an observation that is further supported by the recent discovery that alum induces B cell priming and Ca^{2+} mobilization via a splenic Gr-1$^+$ myeloid IL-4–producing cell type (5). Classical cell-mediated immunity measured by DTH responses and induction of CD8$^+$ CTL responses to a range of polypeptide and protein Ags is poorly induced by alum, caused by a lack of cross-priming (9, 10, 1). However, proliferative responses of CD4$^+$ T cells, as well as Th2 cytokine production, have been found to be enhanced in several murine and human studies, suggesting that alum boosts humoral immunity by providing Th2 cell help to follicular B cells (11, 8, 2).

DCs are seen as nature's adjuvant and have the potential to recognize foreign Ag, process it into small peptides for presentation onto MHC molecules to the TCR, and provide the essential costimulatory molecules for activation of naive CD4$^+$ and CD8$^+$ T cells (12). DCs have an immature phenotype in peripheral tissues, specialized for Ag uptake, but upon recognition of exogenous or endogenous "danger signals" like uric acid or extracellular ATP, they migrate to the LN T cell paracortex, where they arrive

M. Kool, T. Soullié, H. Hammad, and B.N. Lambrecht contributed equally to this paper.
The online version of this article contains supplemental material.

as mature cells, expressing all costimulatory molecules and having lost the capacity to take up Ags (13, 14). The response of DCs to exposure to foreign Ags is part of the innate immune response, and by providing a link between Ag recognition and Ag processing for presentation to naive T cells, these cells bridge innate and adaptive immunity (15).

Many agents with adjuvant activity, such as bacterial endotoxin, Freund's adjuvant, bacterial CpG motifs, monophosphoryl lipid A, MF59, and α-galactosylceramide boost immunity through induction of DC maturation (16–19). It has been less clear if and how aluminum-containing adjuvants can induce DC mobilization and maturation. At least in vitro, alum did not enhance costimulatory molecule expression and DC maturation, although this finding would not preclude such an effect in vivo, as endogenously released danger signals from damaged or inflammatory cells might indirectly activate DCs (20, 21, 13). The issue is even more complex as Toll-like receptors and TLR signaling through the MyD88 or TRIF adaptor pathway, classical activators of innate immunity and the DC network in vivo, were not always necessary for alum to act as an adjuvant for humoral immunity (6, 22, 21). In view of the crucial role of DCs in activation of adaptive immunity, we therefore set out to carefully study the effects of alum on DCs and their monocytic precursors in vivo after i.p. and i.m. injection of antigen (Ag) in alum and studied T cell activation using an adoptive transfer system of traceable Ag-specific T cells. Our experiments revealed a hitherto unappreciated role for monocyte-derived inflammatory DCs and uric acid release in boosting adaptive immunity in alum-formulated Ag preparations.

RESULTS

Distribution of the primary immune response after i.p. injection of OVA

Despite the wide use of i.p. injection of experimental Ags coupled to alum adjuvant, the precise localization of primary T cell activation after i.p. injection of Ag has not been studied in great detail. By analogy with the rapid resorption of drugs after i.p. injection, it is often assumed that i.p. injection leads to rapid systemic resorption of Ag, and therefore i.p. injection is often regarded as systemic immunization. To study primary T cell activation, naive BALB/c mice received a cohort of CFSE-labeled OVA-specific TCR Tg cells obtained from DO11.10 mice, and mice were subsequently immunized 1 d later with 10 μg of OVA via an i.p. injection in the right lower quadrant. 2 d later, primary T cell divisions were readily noticed in the inguinal LN (ILN) on the right side, and in the mediastinal LN (MLN). In Ag-injected mice, only the $CD4^+$ Ag-specific T cells recognized by the KJ1-26 Ab divided, whereas a coinjected fraction of TCR Tg population did not. Strikingly, there were no primary divisions in the contralateral left ILN or in the spleen (Fig. 1 A). The fact that Ag presentation occurred only in the ipsilateral ILN was caused by the fact that the needle injection caused a break in the peritoneal and skin barrier. This was clear when we injected the Ag in the left lower quadrant, in which case divisions occurred in the left ILN, or when we combined a right Ag injection with a left sterile puncture containing no Ag, in which case both ILNs reacted to the Ag (Fig. 1 B). When the right ILN was resected before Ag injection on the right side, the ipsilateral axillary LN became Ag reactive, illustrating that the Ag reached the LN via the afferent lymphatics (unpublished data).

When T cell division was followed over time (Fig. S1, available at http://www.jem.org/cgi/content/full/jem.20071087/DC1), it was evident that Ag-specific T cell responses were restricted to the draining right ILN and MLN for the first 3 d of the response. By day 4, cells that had divided at least three times began to appear in the nondraining LNs and, importantly, also in the spleen. These cells expressed high levels of CD44 and low levels of CD69, which is consistent with their phenotype of recirculating primed T cells as previously reported (unpublished data) (23, 24). However, by day 7 and 14, the majority of divided cells had disappeared from the lymphoid organs and could not be retrieved from the peritoneum.

Effect of alum adjuvant on the immune response induced by an i.p. or i.m. injection of OVA

When OVA was emulsified in alum adjuvant, the localization of the primary immune response after i.p. injection into the lower right quadrant was again restricted to the ipsilateral ILN and MLN. In some mice, there was also a clear primary proliferation of OVA-specific TCR Tg cells in the mesenteric nodes, as previously reported for $CD8^+$ T cell responses after i.p. injection (unpublished data) (25). By day 4 of the response, the primary T cell response in the draining MLN (and ILN) was more pronounced in mice receiving both OVA and alum compared with OVA alone, with a total percentage of $CFSE^+$ Tg cells of 1.7 vs. 0.6% in the mediastinal nodes (Fig. 2 A). By day 2–4 of the response, there was a clear increase in CFSE content (i.e., the number of $CFSE^+$ $KJ1\text{-}26^+$ cells per 10^5 $CD4^+$ T cells, correcting for the multiplying effect of cell division) in OVA-alum–immunized mice compared with mice only immunized with OVA or saline control, signifying that the increase was not only caused by division but also by recruitment of naive Ag-specific T cells to these nodes (Fig. 2 B). However, such recruitment did not occur in nondraining nodes. Also, significantly more divided $CFSE^+$ Tg^+ recirculating effector cells were seen in the nondraining node and spleen. By day 7, a time point when the majority of OVA-specific TCR Tg T cells have disappeared in mice receiving OVA, the Tg T cells persisted in the draining and nondraining nodes and spleen in mice receiving OVA-alum (Fig. 2, A [right] and B). These persisting cells in the mediastinal nodes had Th2 effector potential in the OVA-alum group, as they produced IL-4, -5, and -10, but little IFNγ (Fig. 2 C). Bulk cultures of mediastinal node cells from OVA-immunized mice did not produce significant levels of cytokines in response to OVA

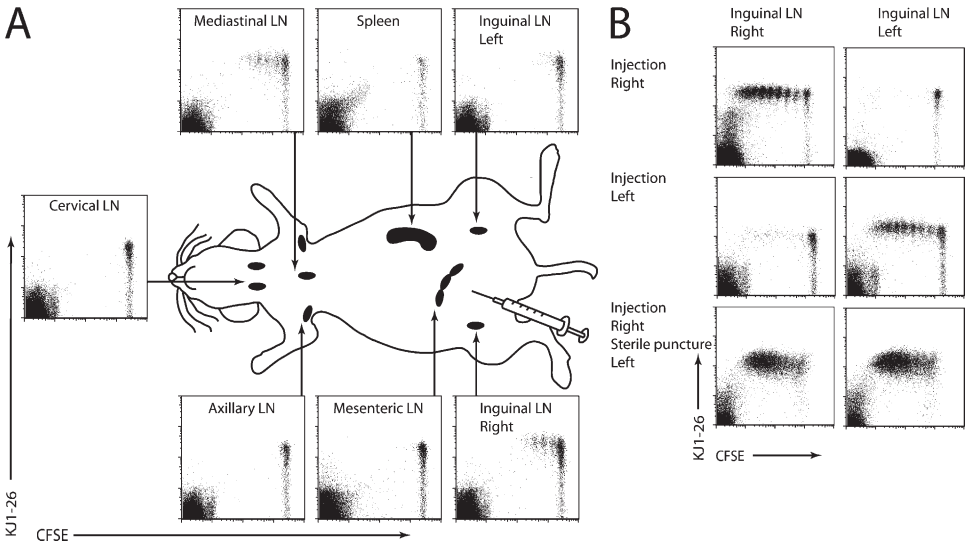

Figure 1. The mediastinal and ipsilateral ILN drain the peritoneal cavity after i.p. injection. Mice were injected with CFSE-labeled DO11.10 OVA-TCR Tg cells 1 d before the i.p. injection of OVA in the right lower quadrant. (A) 2 d after OVA injection, different LNs and spleen were taken and T cell proliferation was assessed with flow cytometry after CFSE dilution. Only KJ1-26 Ag-reactive T cells divide. (B) Immediately after the administration of OVA in the right lower quadrant, a sterile puncture was made at the left lower quadrant. 4 d later, proliferation was measured in the left and right ILN. An example is shown of four mice (representative of at least two independent experiments).

restimulation. In the nondraining nodes, there was similarly a clear increase in Th2 cytokine production in mice receiving OVA-alum, most likely caused by recirculating primed T cells.

The i.p. route is most often used for immunization of animals because of its ease of use, but in humans, most alum-formulated adjuvants are injected i.m. or s.c. We therefore also studied the response to OVA-alum and OVA after i.m. injection into the gluteal muscle of mice. In these mice, the primary DLN site was the sacral LN. Again, OVA injection alone led to transient T cell activation followed by deletion of dividing cells, whereas alum injection left behind a persistent and recirculating T cell response, which was most prominent in the sacral node (Fig. S2 A, available at http://www.jem.org/cgi/content/full/jem.20071087/DC1).

Response of innate immune system cells to i.p. injection of Ag in adjuvant

Having identified the MLN as the most physiological draining site after i.p. injection of Ag in alum, we next directed our interest to the innate immune response to adjuvant in the peritoneum and how cells would take up and translocate Ag from the peritoneum to this node. By analogy with other adjuvants, it is possible that alum adjuvant is immunogenic because of its induction of inflammation at the site of injection, thus recruiting APCs to the site of Ag exposure (7). One of the most prominent cell types found in the peritoneal cavity of unimmunized mice are the resident $F4/80^{high}CD11b^{high}$ peritoneal macrophages. Within 6 h after injection, there was a dramatic reduction in these resident macrophages in mice receiving OVA-alum, but not OVA (Fig. 3 A). On the contrary, OVA-alum induced a rapid recruitment into the peritoneal cavity of $CD11b^{+}F4/80^{int}Ly6G^{-}Ly6C^{high}$ inflammatory monocytes, previously shown to be immediate precursors for DCs (26, 27). 12 and 24 h after injection of OVA-alum, a significant increase in the number of myeloid DCs (defined as $MHCII^{high}CD11c^{+}F4/80^{low}$) and plasmacytoid DCs (defined as $120G8^{+}CD11b^{dim}CD11c^{int}$) could be found compared with OVA-injected mice. Furthermore, OVA-alum led to a marked increase in the numbers of neutrophils (defined as $CD11b^{+}Ly6C^{+}Ly6G^{high}F4/80^{-}$ cells) and eosinophils ($CD11b^{+}Ly6C^{dim}Ly6G^{dim}F4/80^{dim}$) recruited into the peritoneal cavity. In an attempt to explain the increase in innate immune cells so early after injection of alum, we also measured the levels of chemokines in the peritoneal lavage at 2 h after injection of saline, OVA, or OVA-alum. There was a marked increase in the levels of the monocyte chemotactic protein (MCP1; CCL2), the neutrophil chemotaxin KC (CXCL1), and the eosinophil chemotaxin eotaxin-1 (CCL11) in mice receiving OVA-alum versus OVA or saline (Fig. 3 B). OVA by itself induced an intermediate level of MCP-1 compared with saline- or OVA-alum–injected mice.

At 24 h after injection, we also studied the presence of a population of IL-4–producing $Gr\text{-}1^{+}$ myeloid cells, which were previously shown to be involved in inducing splenic B cell priming after alum injection (5). Using IL-4 GFP reporter mice (4-Get mice) (28), we could detect an alum-induced increase in this population in the peritoneum and spleen, but not MLNs. In addition, we found that alum induced two populations of $CD11b^{+}Gr1^{+}$ myeloid cells expressing IL-4 in the peritoneum, the highest $Gr1^{+}$ one most likely being granular $F4/80^{+}$ eosinophils, and the intermediate Gr1-expressing one being monocytes (Fig. S3, available at http://www.jem.org/cgi/content/full/jem.20071087/DC1).

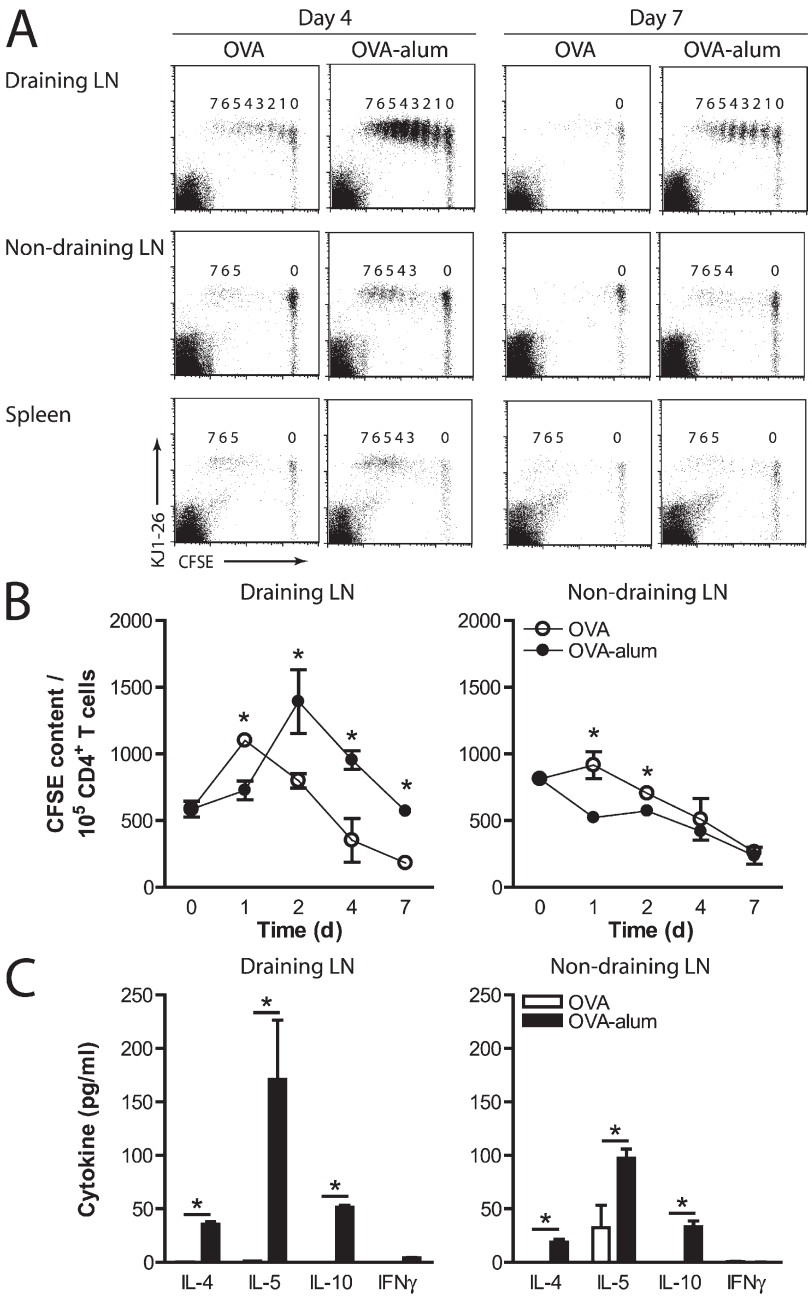

Figure 2. Addition of alum adjuvant to OVA leads to a stronger, more persistent and recirculating Th2 immune response. Mice were injected with CFSE-labeled DO11.10 OVA-TCR Tg cells 1 d before the i.p. injection of OVA or OVA-alum. (A) 4 and 7 d after the injection the DLN (MLN), nondraining LN (CLN), and the spleen were analyzed for T cell proliferation with flow cytometry (n = 4 mice; experiment performed three times). (B) CFSE content was calculated as described in Materials and methods, and is shown for DLN (MLN) and nondraining LN (ALN). Open symbols represent the OVA-injected mice, and the filled symbols the OVA-alum injected mice. (C) 7 d after the i.p. injection, LN cells (DLN: MLN, nondraining LN: ALN) were taken and restimulated in vitro for 4 d with OVA. Cytokines were measured in the supernatants by ELISA. Open bars represent OVA-injected mice, and closed bars represent the OVA-alum–injected mice. Data are shown as the mean ± the SEM, *, $P < 0.05$. n = 4–6 mice per group.

Ag uptake and processing by recruited DCs

The increase in DCs after injection of OVA-alum led us to study the effects of alum on several functional aspects of DCs, including Ag uptake, processing, and functional maturation. To investigate if alum had an effect on the Ag uptake by DCs, OVA-Alexa Fluor 647 was injected i.p. either alone or emulsified in alum and uptake by $CD11c^+$ DCs in the peritoneal cavity was measured 6 and 24 h later. Even in the absence of alum, DCs captured the Ag, but the mean fluorescence intensity representing the amount of Ag taken up was higher when alum was added (Fig. 4 A, results at 24 h are shown). Under the same conditions, peritoneal B cells also took up more fluorescent Ag

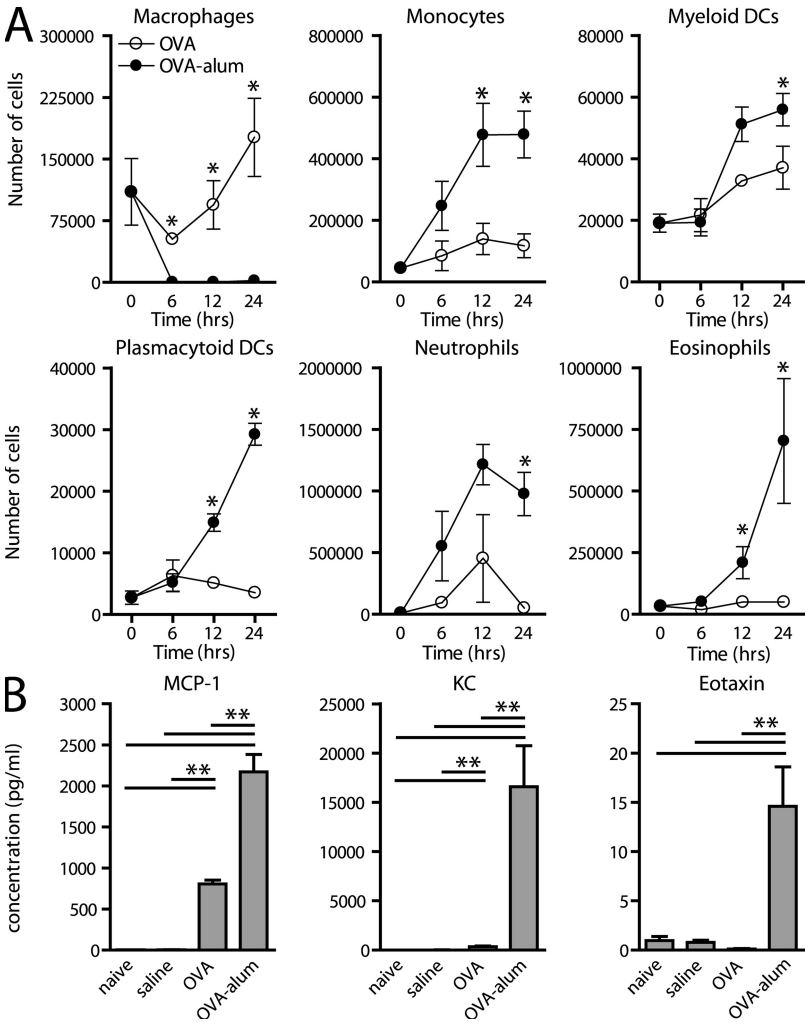

Figure 3. Alum recruits innate immune cells to the peritoneal cavity. Mice were injected i.p. with OVA or OVA alum. (A) 6, 12, and 24 h after injection, the peritoneal lavage was taken and the number of macrophages ($F4/80^{high}CD11b^{+}SSC^{high}$), monocytes ($CD11b^{+}Ly6C^{high}Ly6G^{-}F4/80^{int}$), myeloid DCs ($MHCII^{high}CD11c^{+}F4/80^{low}$), plasmacytoid DCs ($120G8^{+}CD11b^{dim}CD11c^{int}$), neutrophils ($CD11b^{+}Ly6C^{+}Ly6G^{high}F4/80^{-}$), and eosinophils ($CD11b^{+}Ly6C^{int}Ly6G^{int}F4/80^{int}$) was determined. Open symbols represent the OVA-injected mice, and filled symbols the OVA-alum injected mice. (B) 2 h after injection, the peritoneal lavage was taken and chemokine levels were determined in the supernatant by ELISA. Data shown are the mean ± the SEM. *, $P < 0.05$. $n = 4–6$ mice per group.

when alum was added, whereas recruited eosinophils and neutrophils did not take up OVA-Alexa Fluor 647, even in the presence of alum (unpublished data).

To analyze Ag processing of internalized Ag, we used OVA-DQ, a form of OVA that is highly conjugated to the BODIPY fluorochrome that fluoresces in the green channel when taken up by cells and in the red channel when it accumulates at high densities inside endosomal Ag-processing compartments. $CD11c^{+}MHCII^{+}$ DCs from OVA-DQ–alum treated mice took up and processed more Ag than OVA-DQ–treated mice (Fig. 4 B). When the $CD11c^{+}OVA\text{-}DQ^{double\ pos}$ cells were analyzed in the OVA-DQ-alum–treated mice, they expressed more MHC class II than the $OVA\text{-}DQ^{neg}$ cells, indicating that the DCs that took up and processed Ag also functionally matured (Fig. 4 C). After injection of OVA-alum, we observed that the DC maturation marker CD86 (and CD40; unpublished data) was induced on peritoneal lavage $CD11c^{+}MHCII^{+}$ DCs within 6 h, and started to return to baseline from 24 h onwards compared with an injection of OVA or saline (Fig. 4 D). This effect of alum on DC maturation was most likely indirect, as exposure of purified BM-derived DCs to alum in vitro did not lead to any direct DC activation (Fig. 4 D, right) (20, 21). The ultimate definition of DC function is the potential to present Ag to naive T cells. When $CD11c^{+}MHCII^{+}$ DCs were sorted from the peritoneum of immunized mice, only DCs derived from OVA-alum–immunized mice induced T cell proliferation of naive DO11.10 OVA-specific T cells ex vivo (Fig. 4 E), which is best explained by induction of DC maturation (Fig. 4 D) and more efficient Ag processing by these cells (Fig. 4 B).

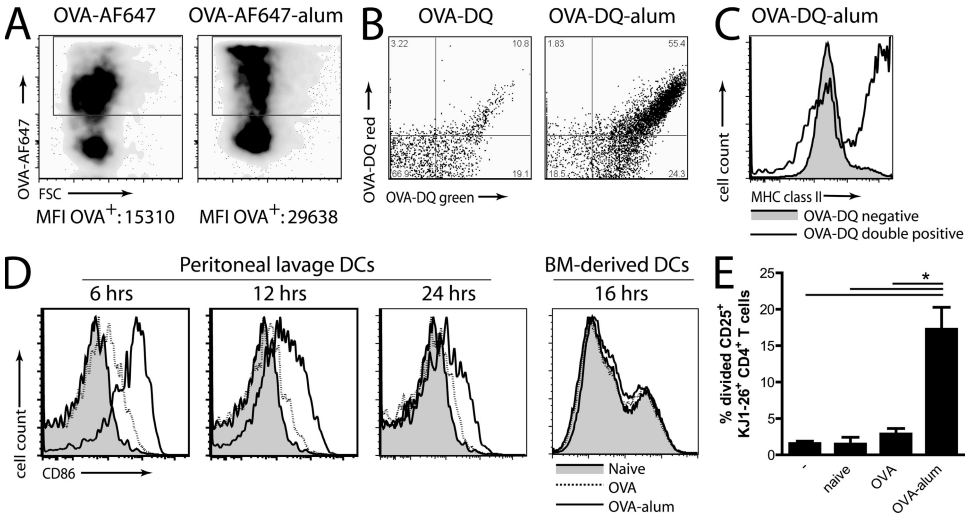

Figure 4. Alum adjuvant stimulates DC function in vivo. (A) Mice were injected i.p. with OVA-Alexa Fluor 647 (OVA-AF647) or OVA-AF647-alum. 24 h after injection, the peritoneal lavage was taken and the uptake of OVA-AF647 was assessed in F4/80$^-$MHCII$^+$CD11c$^+$ DCs. (B) Mice were injected with OVA-DQ or OVA-DQ-alum i.p., and 24 h later, the mDCs (F4/80$^-$MHCII$^+$CD11c$^+$) in the peritoneal lavage were analyzed for the uptake and processing of DQ by flow cytometry. OVA-DQ fluoresces green when processed in acidified lysosomes. Red fluorescence is caused by accumulation of OVA-DQ in endosomal processing compartments in the cell. (C) The CD11c$^+$ cells were also analyzed for the expression of MHCII in the DQ-negative or –double-positive gate. Gray-filled histograms represent OVA-DQ–negative, and black line histograms represent OVA-DQ–double-positive CD11c$^+$ cells. (D) Maturation of mDCs in the peritoneal lavage was assayed 6, 12, and 24 h after injection of OVA or OVA-alum by flow cytometry. BM-derived DCs (BM-DCs) were pulsed for 16 h with OVA or OVA-alum. Gray filled histograms represent naive mice or unpulsed BM-DCs, black dotted line histograms represent OVA-injected mice or OVA-pulsed BM-DCs, and black solid line histograms represent OVA-alum–injected mice or OVA-alum–pulsed BM-DCs. (E) Mice were injected with OVA or OVA-alum, and 6 h later, the F4/80$^-$MHCII$^+$CD11c$^+$ DCs were sorted from the peritoneal lavage and placed in co-culture with CFSE-labeled DO11.10 Tg CD4$^+$ T cells. After 4 d, cells were analyzed for proliferation and gated for CD4$^+$, KJ1-26$^+$, and CD25$^+$.

One aspect of DC biology that cannot be overestimated is their potential to migrate to the DLN. Uptake studies in mice receiving OVA-DQ-alum revealed that within 24 h, 10% of CD11c$^+$MHCII$^+$ DCs in the MLN had taken up Ag and processed it into immunogenic fragments, as did 2% of CD19$^+$MHCII$^+$ B cells and 10% of 120G8$^+$CD11c^{int} pDCs. The addition of alum to OVA led to a strong increase in cells positive for processed OVA-DQ, from 0.05 to 0.87% of all live DLN cells, particularly in DCs and B cells (FACS plots not depicted). We could not detect significant OVA-DQ processing in any APC population in nondraining nodes.

Injection of alum promotes Ag uptake by recruited monocytes and induces their migration and conversion into CD11c$^+$ DCs in the draining nodes

Injection of OVA-alum induced the recruitment of inflammatory CD11b$^+$Ly6G$^-$Ly6C$^+$F4/80^{int} monocytes to the peritoneal cavity (Fig. 3 A). When fluorescent OVA-AF647 was mixed with alum, these inflammatory monocytes massively took up more Ag compared with OVA-AF647 injected alone (Fig. 5 A, top). Particularly in OVA-alum immunized mice, Ly6C^{high}CD11b$^+$monocytes (identified using the same gating strategy as in the peritoneum) carrying fluorescent OVA-Alexa Fluor 647 could also be found in the mediastinal nodes by 24 h after immunization (Fig. 5 A, bottom). Because of incompatible staining reagents, we could not measure OVA-DQ processing in this monocyte subset. To prove that they were processing the internalized Ag, Ly6C$^+$ monocytes were sorted from MLN, and they induced ex vivo proliferation of DO11.10 T cells when obtained from OVA-alum–immunized mice (Fig. 5 B). The T cell division induced by sorted monocytes was even greater than the one induced by sorted MLN DCs (sorted based on classical characteristics). Consistent with the induction of T cell proliferation, monocytes arriving in the MLN and carrying Ag to these nodes (measured by OVA Alexa Fluor 647) acquired costimulatory molecule expression (CD86 and CD40), up-regulated MHCII and most importantly also acquired the CD11c integrin, a classical marker of DCs. These changes were most pronounced in monocytes that had taken up Ag (Fig. 5 C). As these findings were largely descriptive and not excluding the possibility that LN resident monocytes acquired the Ag and up-regulated CD11c in situ, we performed adoptive transfer experiments of flow cytometry sorted Ly6C$^+$CD11b$^+$CD31$^-$ bone marrow monocytes obtained from CD45.2 congenic mice that were injected i.p. into CD45.1 recipients, 2 h after injection of OVA or OVA-alum. As shown in Fig. 5 D, CD45.2 monocytes migrated from the peritoneal cavity to the MLN, and this migration was strongly amplified by the addition of alum. When CD45.2 bone marrow monocytes were phenotyped before i.p. injection, they were negative for the DC markers CD11c and MHC class II. However, CD45.2 monocytes recovered from the MLN 36 h after i.p. injection now strongly expressed MHC class II and CD11c, and up to 25% of cells expressed both markers, indicative of conversion to DCs.

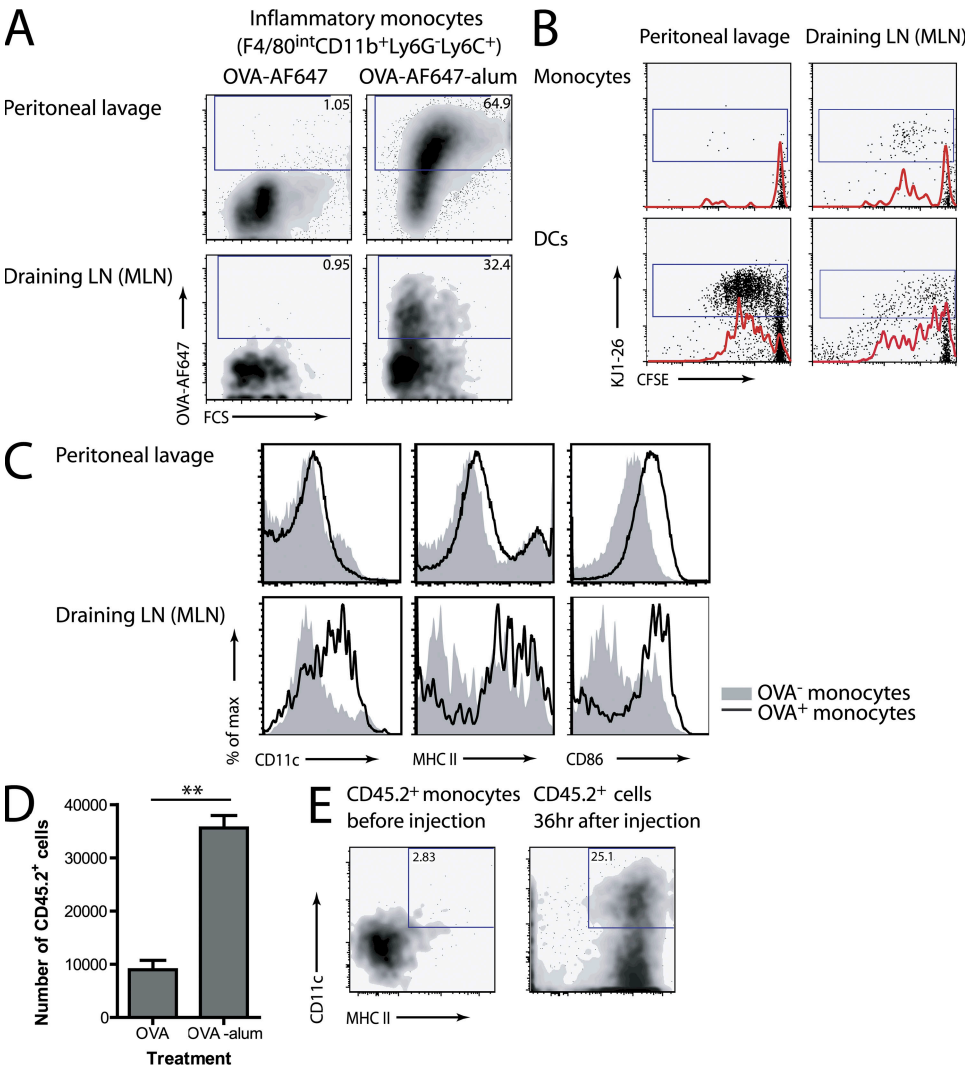

Figure 5. Inflammatory monocytes recruited by alum take up Ag, migrate to DLN and acquire a DC phenotype. Mice were injected with OVA-Alexa Fluor 647 (OVA-AF647) or OVA-AF647-alum, and 24 h later, the peritoneal lavage and DLN (MLN) were taken. (A) Presence of OVA-AF647 in inflammatory monocytes (defined as $CD11b^+Ly6C^{high}Ly6G^-F4/80^{int}$) is shown in the peritoneal lavage and MLN. (B) Inflammatory monocytes and mDCs ($CD11b^+MHCII^{high}Ly6C^-$) were sorted and placed in co-culture with CFSE-labeled DO11.10 Tg $CD4^+$ T cells. T cell proliferation was assayed at day 4 and plots depict PI-negative $CD4^+$ cells. (C) Expression of CD11c, MHC II, and CD86 on inflammatory monocytes determined by nine-color flow cytometry. Gray filled histograms represent the OVA-AF647–negative monocytes, whereas the black line histogram represents the OVA-AF647-positive ones. An example representative of four mice is shown. (D) CD45.1 mice were injected with OVA or OVA-alum. 2 h later, they received $CD45.2^+$ monocytes sorted from bone marrow (purity >95%). 36 h later, the number of $CD45.2^+$ cells in the MLN were determined by flowcytometry. Data shown are the mean ± the SEM. **, $P < 0.01$. $n = 4–5$ mice per group. (E) The CD11c and MHC II expression was assessed on the $CD45.2^+$ cells before injection, and 36 h later, in the MLN.

When we studied the uptake and transport of fluorescent Ag after i.m. injection into the gluteal muscle, we could similarly detect Ag uptake by DCs (Fig. S2 B) and inflammatory monocytes (Fig. S2 C) in the muscle. When OVA-alum was administered, Ag-laden inflammatory monocytes were especially prone to accumulate in higher numbers in the draining sacral nodes.

Functional effect of depleting resident or recruited DCs on T cell priming and humoral immune response induced by OVA or OVA-alum

The i.p. injection of OVA by itself did not lead to peritoneal DC activation and Ag presentation (Fig. 4), nor recruitment of inflammatory Ag laden monocytes to the mediastinal nodes (Fig. 5), yet T cell divisions were induced in these nodes by OVA (Figs. 1, 2, and S1). One possibility would be that i.p. injected Ag reaches the LN via the flow of afferent lymph from the peritoneum in the absence of cell migration. We indeed observed that 2 h after injection of OVA-AF647 with or without alum, the MLN subcapsular sinus and B cell area became strongly fluorescent when we imaged sections directly without hydration (unpublished data), as previously shown by others (29, 30). We therefore hypothesized that in the absence of alum, Ag was presented by resident nonmigratory LN APCs that acquired the Ag via the afferent lymph,

whereas in the presence of alum, Ag was presented by recruited inflammatory monocytes and DCs that migrated to the nodes. To address this hypothesis, we used transgenic mice in which DCs can be conditionally depleted by administration of diphtheria toxin (DT). In these mice the human DTR receptor is expressed under the control of the murine CD11c promotor, leading to the rapid killing of CD11c^{hi} cells upon DT administration (31, 32). Control mice in these experiments were nontransgenic littermates that received a similar treatment with DT. DT was administered locally via the intratracheal (i.t.) route, leading to a depletion of mediastinal-resident LN (Fig. S4, available at http://www.jem.org/cgi/content/full/jem.20071087/DC1), as well as lung-derived migratory DCs, whereas leaving all other DCs unaffected (32). By taking advantage of the unique feature that the MLN drains both the lung and peritoneum, we could deplete

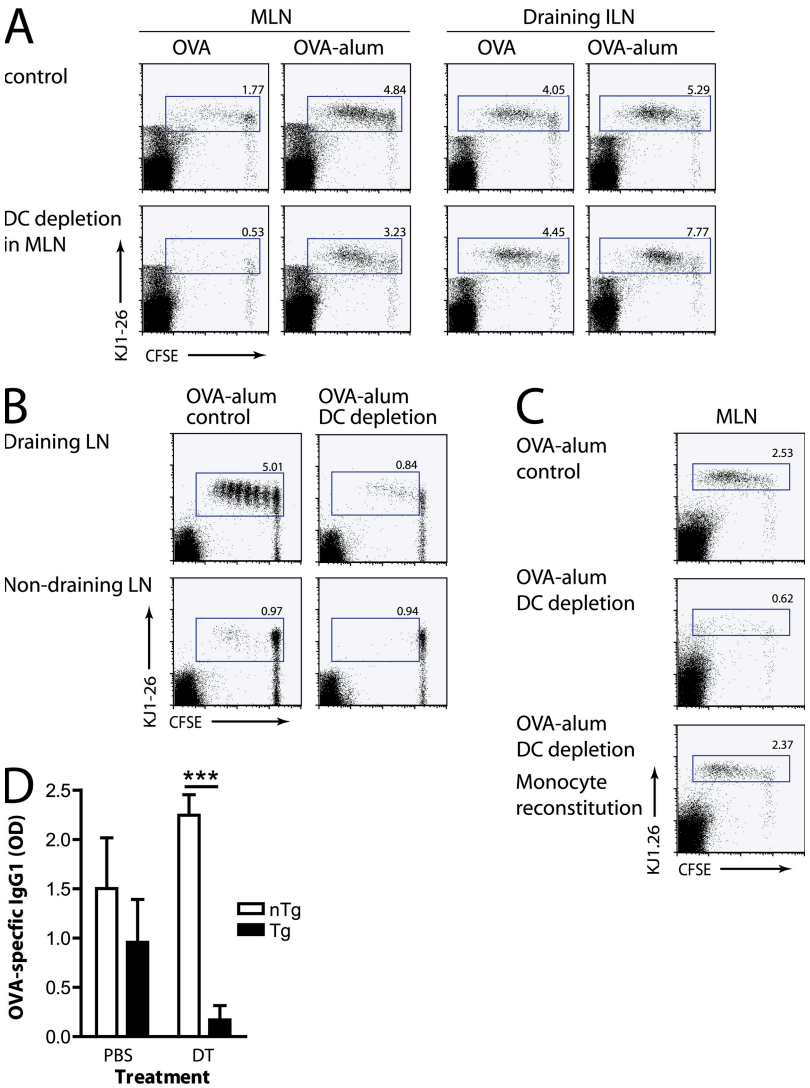

Figure 6. Contribution of resident versus recruited CD11c$^+$ DCs on Ag presentation and immunopotentiating effect of alum adjuvant. (A) CD11c-DTR Tg mice were depleted of resident MLN DCs by an i.t. injection of 100 ng DT or PBS as a control. 1 d before DT, they received a cohort of CFSE-labeled CD4$^+$ DO11.10 T cells i.v. 1 d after DT, OVA or OVA-alum was given i.p. 3 d after the last injection, proliferation of Tg T cells were determined in the draining MLN and draining right ILN. Percentages in the plots are the percentage of Tg cells from total CD4$^+$ T cells. (B) To deplete all CD11c$^+$ cells (resident and recruited) CD11c-DTR Tg mice were injected i.p. with 100 ng DT or PBS as a control. 1 d before DT, they received a cohort of CFSE-labeled CD4$^+$ DO11.10 T cells i.v. OVA or OVA-alum was given i.p. 4 d after the last injection, and proliferation of Tg T cells was determined in the DLN (MLN) and nondraining LN (CLN). Percentages in the plots are the percentage Tg cells from total CD4$^+$ T cells. (C) CD11c-DTR Tg mice were depleted of DCs by an i.p. injection of 100 ng DT or PBS as a control. 1 d before DT, they received a cohort of CFSE-labeled CD4$^+$ DO11.10 T cells i.v. 1 d after DT, OVA, or OVA-alum was given i.p. with or without sorted monocytes from BALB/c mice. 4 d after the last injection, proliferation of Tg CD4$^+$ T cells was determined in the draining MLN. An example is shown in 4 mice; the experiment was repeated at least two times. (D) CD11c-DTR Tg mice and non-Tg mice were injected with PBS or DT and received an i.p. injection of OVA-alum, and 10 d later, serum samples were taken and OVA-specific IgG1 levels were determined by ELISA. Data are shown as the mean ± the SEM, * $P < 0.05$. n = 4–5 mice per group.

LN-resident DCs also draining the peritoneum without having to administer the toxin to the peritoneum. When resident DC-depleted mice received an i.p. injection of Ag 1 d later, T cell proliferation (measured 3 d after injection of OVA) was abolished in the MLN in mice receiving OVA, but not those receiving OVA-alum (Fig. 6 A). On the contrary, the ipsilateral draining ILN still demonstrated T cell proliferation in response to OVA, even when DT was administered to the lung, illustrating that the toxin did not affect resident DC function outside the mediastinal node.

To finally study the function of migratory DCs and monocyte-derived DCs in the priming of the immune system by OVA-alum, we also administered the DT toxin systemically through the peritoneal route, depleting all $CD11c^{hi}$ cells, including the resident ones (31). When CD11c-DTR Tg mice received an i.p. injection of OVA-alum, adoptively transferred DO11.10 T cells divided strongly when $CD11c^{+}$ cells were present (Fig. 6 B). In CD11c-depleted mice, there was a very strong reduction in T cell divisions at day 4 of the response, and there was no occurrence of recirculating divided T cells in the nondraining nodes. As the population of recruited inflammatory $CD11b^{+}Ly6G^{-}Ly6C^{+}F4/80^{int}$ monocytes differentiated into DCs in vivo (Fig. 5 E), we finally tested whether sorted BM-derived monocytes injected i.p. could restore divisions in mice depleted of $CD11c^{hi}$ cells. As shown in Fig. 6 C, injection of monocytes 2 h after injection of OVA-alum restored T cell divisions in Ag-specific T cells in the MLN of mice depleted of DCs.

Aluminum adjuvant is widely used for its strong induction of the humoral response, possibly through induction of direct priming of B cells by a myeloid IL-4–producing cell type (5) and by induction of T cell help for class switching. To examine if the humoral response would also be dependent on DCs, we treated CD11c-DTR mice or non-Tg littermates with DT and injected them with OVA-alum. 10 d after the injection, serum samples were taken and OVA-specific IgG1 and IgE levels were determined. In DC-depleted mice (CD11c-DTR Tg mice given DT) a significant reduction in the levels of OVA-specific IgG1 was found (Fig. 6 D). OVA-specific IgE levels in serum also showed this trend, although it did not reach significance (unpublished data).

The immunopotentiating effect of alum depends on induction of uric acid and signaling through the MyD88 pathway

The fact that monocytes are recruited to the peritoneum and differentiate into full-blown Ag-presenting DCs does not explain how these cells get activated. One striking finding was that alum induced a strong neutrophilic influx, accompanied by the production of CXCL1 (KC) and CCL2 (MCP-1; Fig. 3), as well as IL-1β and -18 (not depicted) (21), akin to the response seen when the endogenous danger signal uric acid is injected into the peritoneal cavity (33, 34). We therefore measured the level of uric acid in the peritoneal lavage 6 h after injection of saline, OVA, or OVA-alum and found that only alum induced a strong increase in uric acid levels (Fig. 7 A). To test the functional significance of this induced uric acid, we neutralized it by treating mice with the uric acid–degrading enzyme uricase before administration of OVA–Alexa Fluor 647 in the presence or absence of alum. The recruitment of OVA-laden $CD11b^{+}Ly6G^{-}Ly6C^{+}F4/80^{int}$ inflammatory monocytes to the MLN was completely abolished in mice treated with uricase (Fig. 7 B), and consequently, T cell division that is normally avidly induced in vivo in the presence of alum was abolished back to the control level when uricase was given (Fig. 7, C and D). It was previously shown that the peritoneal response to uric acid is heavily dependent on the IL-1 receptor and downstream MyD88 signaling. To test this possibility, we gave OVA-Alexa Fluor $647^{+/-}$ alum to $MyD88^{-/-}$ C57BL/6 mice and found that the recruitment of inflammatory monocytes to the MLN was grossly reduced compared with WT animals (Fig. 7 E).

DISCUSSION

By carefully studying the kinetics and distribution of the innate and adaptive T cell immune response after i.p. injection of OVA in alum, we have uncovered a previously unappreciated role for monocyte-derived DCs in mediating the adjuvant effects of alum on cellular and humoral immunity. This is underscored by the fact that inflammatory monocytes and DCs were attracted to the peritoneum after injection of OVA-alum; that they took up and processed the Ag on their way to the MLNs; that they acquired a functional phenotype of mature DCs once in the LN; and, finally, that removal of $CD11c^{+}$ DCs abolished T cell proliferation in OVA-alum–immunized mice, an effect that was restored by adoptive transfer of $Ly6C^{hi}$ monocytes.

One of the aspects of our study that allowed us to uncover this new mechanism of action of alum was the assessment of the precise localization where Ag presentation occurred after i.p. injection. The peritoneal route is easily accessible and often used as a site for immunization to test the protective effect of novel vaccines against subsequent infection. The good resorption of drugs from the peritoneal cavity has mislead the immunological community, as it is often assumed that i.p. administration of a protein Ag leads to rapid systemic resorption into the bloodstream, leading to the common notion that i.p. administered Ags are presented by APCs in the spleen, similar to i.v. injected Ags. Therefore, i.p. immunization is often equalled to "systemic immunization," and investigators studying the immunogenicity of alum have focused on the spleen as a site where immune activation might occur (22, 5). We show that i.p. injection of the OVA Ag in the right lower quadrant of the peritoneal cavity leads to Ag presentation and Ag-induced T cell proliferation in the MLN and the ipsilateral ILN, but not in the spleen. After T cell divisions over time, it was clear that only after 4 d, when T cells had undergone at least 3–4 divisions, could we detect divided cells in nondraining LNs and spleen, very similar to what we and others described for immunization with Ags via the skin or respiratory mucosa (23). Therefore, the Ag-specific reactivity that can be measured in the spleen ex vivo is the result

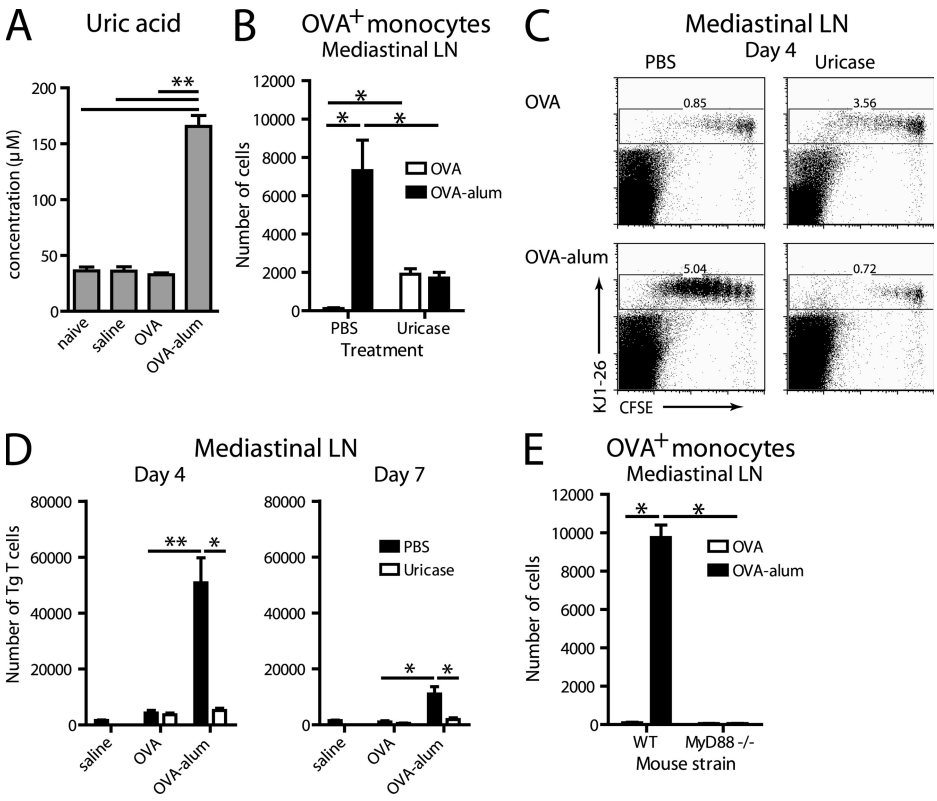

Figure 7. The alum response in mice depends on uric acid and MyD88 signaling. (A) Mice were injected with saline, OVA, or OVA-alum, and after 2 h, uric acid levels were determined in the peritoneal lavage. Data are shown as the mean ± the SEM. **, $P < 0.01$. n = 5–6 mice per group. (B) Mice were injected with uricase 1 d and 5 min before OVA-AF647 or OVA-AF647-alum, and 24 h later, the DLNs (MLN) were taken. The number of OVA-AF647$^+$ inflammatory monocytes (defined as CD11b$^+$Ly6C^{high}Ly6G$^-$F4/80^{int}) are shown. Data are shown as the mean ± the SEM. *, $P < 0.05$. n = 4–5 mice per group. (C) At day 0, mice received a cohort of CFSE-labeled DO11.10 T cells i.v. and uricase i.p. At day 1, mice received another injection with uricase, and 5 min thereafter OVA or OVA-alum i.p. 4 d after the last injection, proliferation of Tg T cells were determined in the draining MLN. Percentages in the plots are the percentage of Tg cells from total CD4$^+$ T cells. An example is shown from four mice, and the experiment was repeated twice. (D) Quantification of the number of Tg cells from 4 and 7 d after OVA or OVA-alum plotted in C. Data are shown as mean ± SEM. *, $P < 0.05$; **, $P < 0.01$. n = 4 mice per group. (E) MyD88$^{-/-}$ and WT mice were injected with OVA-AF647 or OVA-AF647-alum, and 24 h later, the DLN (MLN) were examined. The number of OVA-AF647$^+$ inflammatory monocytes (defined as CD11b$^+$Ly6C^{high}Ly6G$^-$F4/80^{int}) are shown. Data are shown as mean ± SEM. *, $P < 0.05$. n = 4 mice per group.

of recirculating effector and/or memory cells. This finding does not exclude that there is immune activation occurring in the spleen before day 3–4 of the response. Within 24 h of injection of OVA-alum, there was induction in the spleen of an IL-4–producing Gr1$^+$ myeloid cell, as described before by others 6 d after injection of alum (5). The induction of divisions in the ipsilateral ILN was unexpected, but was caused by an artifact induced by skin puncture. One important lesson is that ILN nodes should not be taken as "control nondraining nodes," as is often done because of their easy accessibility for Ags that are injected i.p.

It was less surprising that Ag was presented in the MLN as previous studies in rat, mice, and sheep have shown that the peritoneal cavity has a lymphatic drainage consisting of stomata that cross the diaphragm and drain into the parathymic LN and MLN (35, 36, 26). The transport of Ag could be either through free-flowing lymph, gaining access to the subcapsular sinus and conduit system of MLNs and thus to resident DCs and to follicular B cells (29, 37, 30), or it could be mediated by DCs or other APCs that pick up Ag in the peritoneal cavity and migrate to these nodes (38). Both scenarios might come into play. By visualizing unhydrated LN slides, we could detect a massive amount of fluorescent Ag in the MLN within 2 h after i.p. injection, irrespective of whether alum was added or not, which would never be caused by cell transport alone. Cell-mediated transport by inflammatory Ly6C^{high} monocytes and DCs occurred especially when alum was added.

What is the reason for the dramatic difference in T cell outcome when alum adjuvant is added to an Ag? We demonstrated that in the absence of alum, Ag was presented predominantly by nonmigratory LN-resident DCs that acquired the Ag via afferent lymph, as evidenced in experiments in which these resident DCs were depleted locally in the mediastinal node before OVA administration (Fig. 6 A). Itano et al. demonstrated that after skin puncture, there is a rapid flux of cell-free Ag from the site of injection to the skin-draining node, leading to T cell divisions in Ag-specific

T cells, without generation of T cell effector potential (37). We speculate that the physiological drainage of the peritoneal cavity through the stomata in the diaphragm also leads to presentation of Ag in a tolerogenic form by immature resident DCs, inducing deletional T cell proliferation (39, 40). In contrast, when inflammation is induced by alum, there is additional recruitment of inflammatory monocytes and activation of already resident peritoneal DCs that migrate to the LN and arrive as $CD11c^+$ mature cells expressing the necessary costimulatory molecules for naive T cell activation and generation of memory cells (41). Several groups have recently shown that $CCR2^+Ly6C^+$ monocytes are the immediate precursors of inflammatory type DCs, also called "TIP"-DCs under conditions of *Listeria monocytogenes* infection (42), with an enhanced potential to induce effector T cells (27, 43, 44). We believe that our data support the notion that alum boosts immunity by inducing these "inflammatory" DCs. When the resident LN DCs were depleted in the MLN using lung application of a selective DC-depleting DT (32), the induction of T cell division by OVA-alum was not suppressed, whereas when these inflammatory monocytes and DCs were depleted using peritoneal administration of the toxin (31), almost all T cell division disappeared (Fig. 6 B) and there was no longer any priming for humoral immune responses (Fig. 6 D). The effects of DC depletion on T cell division were, however, completely restored when we performed an adoptive transfer of bone marrow–derived $Ly6C^+$ monocytes, cells that acquired a DC phenotype after arrival in the MLN. These data suggest that inflammatory DCs are strongly involved in mediating the enhancing effects of alum on adaptive immunity, and also demonstrate that uptake and processing by other APCs is not sufficient for generating immunity in the absence of DCs. This change of function in monocytes could be the result of their phagocytosis of particulate alum particles, as previously shown for phagocytosis of latex beads injected into the peritoneal cavity (26). One striking feature was that all APCs contained more intracellular Ag when it was emulsified in alum (Figs. 4 and 5, and not depicted for B cells). Particularly in monocytes, the cells that had internalized Ag demonstrated the shift in CD11c, costimulatory molecules, and MHCII, suggesting that Ag uptake was indeed associated with DC differentiation. Inflammatory monocytes in the peritoneum contained fluorescent Ag by 6 h, whereas the same cells were found in the MLN only by 24 h, suggesting migration to these nodes, a finding that is also supported by adoptive transfer experiments of CD45.2 congenic donors.

As our own in vitro experiments (Fig. 4 D) and experiments by others (20) did not reveal a direct activation of monocytes and DCs by alum, we hypothesized that an endogenous danger signal might be released after injection of alum in vivo. We measured very high levels of the endogenous danger signal uric acid when alum was injected and more importantly, recruitment of neutrophils, inflammatory monocytes, and T cell activation induced by alum in the mediastinal LN was abolished when uric acid was neutralized by uricase treatment. Uric acid is released by necrotic cells and alum has been shown to induce a considerable degree of necrosis. It is well known that alum injection i.p. leads to cell death and, when injected into muscle alum, leads to myofascitis. The release of uric acid could explain the high degree of neutrophilic inflammation, as well as CXCL1 production, as a very similar response is seen when uric acid is injected i.p. (13, 33). Moreover, work by others (21), along with our own unpublished work (unpublished data), demonstrated that alum, like uric acid, activates caspase-1 and leads to the release of IL-1β and -18 (33). In support of a predominant role for this pathway in activating inflammatory DCs, we found that the alum response was abrogated in mice deficient in the signaling molecule MyD88, involved in transducing signaling from the IL-1 and -18 receptor. What we cannot presently explain, however, is the fact that the humoral immune response measured several weeks after injection of alum is variably dependent on MyD88 and/or IL1 (6, 45, 46). Although these differences might depend on timing of analysis and contamination or addition of different TLR ligands to alum, it could also be that for induction of humoral responses, IL-1 signaling via Myd88 is redundant, whereas for T cell responses it is crucial (8).

Whether uric acid is the only endogenous innate trigger for DC activation remains to be shown, but the fact that uricase was so effective points toward a predominant role for it. Just like uric acid, alum adjuvant can activate several other aspects of innate immunity, including activation of the coagulation and complement cascade, which is known to influence DC function (7, 47). As alum does not activate bone marrow–derived DCs in vitro, it is tempting to speculate that nonhematopoietic structural cells of the peritoneal cavity might undergo necrosis and subsequently release uric acid, although formal proof of this is lacking. The rapid recruitment of neutrophils and eosinophils within 6 h, along with DCs, could subsequently be responsible for the indirect activation of DCs. Indeed, neutrophils have been shown to activate DCs through CD11b–DC–SIGN interactions, leading to secretion of chemokines and cytokines (48). Whether eosinophils could perform the same task is unclear at present, but they could certainly represent an early source of Th2-polarizing cytokines, which are necessary for Th2 induction by alum (28). It has been shown that alum induces a $Gr\text{-}1^+IL\text{-}4^+$ myeloid population (eosinophils and monocytes) in the spleen 10 d after injection (5). We did see an increase in $Gr1^+IL4^+$ cells in the peritoneum and spleen, but not MLN, within 24 h after injection of alum, but do not know at present whether this population could be involved in activation of the monocytes and DCs.

In conclusion, through a series of in vivo experiments, we showed that alum adjuvant promotes adaptive immunity by releasing the endogenous danger signal uric acid, thus inducing the differentiation of nature's adjuvant, the inflammatory DC, from recruited monocytes.

MATERIALS AND METHODS

Mice. BALB/c mice (6–8 wk old) were purchased from Harlan. OVA-TCR transgenic mice (DO11.10), CD11c-DTR transgenic mice on a BALB/c

background (31), CD45.1, and CD45.2 C57BL/6 mice were bred at Erasmus University (Rotterdam, Netherlands). MyD88$^{-/-}$ mice were provided by B. Ryffel (Centre National de la Recherche, UMR6218, Orleans, France) and originally made by S. Akira (Osaka University, Osaka, Japan). All experiments were approved by the animal ethics committee at the Erasmus Medical Centre.

Ags and adjuvant. OVA was purchased from Worthington Biochemical Corp. At the dose used in our experiments, the endotoxin level of OVA measured by a limulus-amebocyte lysate assay (Biowhittaker) was <0.001 μg/ml. Imject alum (Pierce Biochemicals) is a mixture of aluminum hydroxide and magnesium hydroxide and was mixed at a 1:20 ratio with a solution of OVA Ag in saline, followed by stirring for at least 1 h. For immunization, 500 μl of Imject alum suspension (1 mg) containing 10 μg of OVA (OVA-alum) was injected i.p. in the right lower quadrant using a 26-gauge needle, or alternatively, 10 μg of OVA in 500 μl saline was injected.

Detection of the primary T cell response to i.p. injection of OVA. OVA-specific TCR Tg T cells were collected from the lymphoid organs of naive 4–6 wk old DO11.10 mice and stained with CFSE (Invitrogen) as previously described (23). 10×10^6 cells were injected i.v. in the lateral tail vein of BALB/c mice (day −1). On day 0, the mice received an i.p. injection of 10 μg OVA, OVA-alum, saline, or alum. On day 0, 1, 2, 4, 7, and 14 cervical LNs (CLN), axillary (A)LNs, ILNs, mesenteric (Mes)LNs, MLNs, and spleens were removed, and individual cell suspensions were prepared as previously described (23).

In experiments to address the functional role of DCs in peritoneal responses, CD11c$^+$ cells were depleted by injecting 100 ng of DT either i.t. or i.p. in CD11c-DTR Tg mice (31, 32). In these mice, CD4$^+$ T cells were purified from OVA-specific TCR DO11.10 cells using magnetic separation (CD4$^+$ T Cell Isolation kit; Miltenyi Biotec), and $2–5 \times 10^6$ cells were injected i.v.

In experiments to address if monocytes could restore the phenotype in the DT-treated CD11c-DTR Tg mice, 7.5×10^5 CD11b$^+$Ly6C$^+$CD31$^-$ monocytes sorted from bone marrow of BALB/c mice were injected i.p. 2 h after OVA or OVA-alum injection.

In separate experiments, the i.m. route of administration was investigated by giving 10 μg OVA coupled to 1 mg alum in 50 μl in the left hind limb. 4 and 7 d after the injection, the sacral (S)LNs, popliteal (P)LNs, ILNs, and muscles were removed and prepared for single cell suspensions.

Effector cytokine production. LN and spleen cells (200,000 cells/well in triplicates) were resuspended in culture medium in 96-well plates. 4 d later, supernatants were harvested and analyzed for the presence of cytokines by ELISA (IL-4 and -5 was obtained from eBioscience; IL-10 and IFNγ was obtained from BD Biosciences).

Chemokine production. The peritoneal lavage was taken 2 h after injection of 10 μg OVA, OVA-alum, or saline to determine levels of different chemokines in the supernatant by ELISA (MCP-1 and KC fro was obtained from R&D Systems; eotaxin was obtained from eBioscience).

Flow cytometry. For detection of OVA-specific T cell responses, cells were gated for live (PI-negative) lymphocytes with CD4-APC and the clonotypic anti-OVA TCR antibody KJ1-26-PE. To acquire clear CFSE division profiles, $2.5–10 \times 10^5$ events were collected. The term "CFSE content" gives an estimate of the original number of CFSE-labeled donor cells from which the donor-derived, divided population has arisen and was calculated as previously described (23). It can be used to calculate whether the number of cells at the analyzed site has been affected by recruitment, migration, or cell death, in addition to division.

For detection and sorting of DCs and monocytes, single-cell suspensions of LNs or peritoneal lavage were prepared as previously described (49) or prepared from bone marrow cultures. Cells were subsequently stained with mAbs directed against CD11c, CD11b, MHCII, CD80, CD86, CD40 (eBioscience), F4/80, Ly6C, or Ly6G (BD Biosciences) and with pDC-specific mAb 120G8 (provided by C. Asselin-Paturel, Schering-Plough, Dardilly, France). Sorting of CD11c$^+$ MHCII$^+$ DCs, F4/80^{int}CD11b$^+$Ly6G$^-$Ly6C$^+$ inflammatory monocytes, and F4/80$^+$CD11b$^+$ macrophages was performed on a FACSAria high-speed sorter (BD Biosciences).

For Ag uptake and processing studies, 10 μg of OVA-Alexa Fluor 647 or OVA-DQ (Invitrogen) was coupled or not to Imject alum, injected i.p., and detected 24 h later in the peritoneal cavity or various nodes. Peritoneal lavage and LN cells were stained for seven or nine color flow cytometry using combinations of live (DAPI-negative), Ly6C-FITC and Ly6G-PE or CD19-PE, mPDCA1-APC, CD8-PerCP-Cy5.5 or CD11b-PerCP-Cy5.5, CD11c-PE-Texas red, Ly6G-PE-Cy7 or CD8α-PE-Cy7, MHCII-biotin, or F4/80-biotin, followed by streptavidin-APC-Cy7, CD11b-Pacific blue, combined with uptake of fluorescent Ags of OVA-DQ or OVA-Alexa Fluor 647.

Acquisition of four color samples was on a FACSCalibur cytometer equipped with CellQuest software and seven to nine color samples on a FACSAria cytometer equipped with FACSDiva software (all BD Biosciences). Final analysis and graphical output were performed using FlowJo software (Tree Star, Inc.).

Generation of BM-DCs. Bone marrow cells were cultured for 9 d in DC culture medium (DC-CM; RPMI 1640 containing GlutaMAX-I; Invitrogen) supplemented with 5% (vol/vol) FCS (Sigma-Aldrich), 50 μM 2-mercaptoethanol (Sigma-Aldrich), 50 μg/ml gentamicin (Invitrogen), and 20 ng/ml recombinant mouse GM-CSF (a gift from K. Thielemans, Vrije Universiteit Brussel, Brussels, Belgium). 16 h before harvesting, DCs were exposed either to 10 μg/ml of OVA, alum, or OVA-alum suspension.

Statistical analysis. For all experiments, the difference between groups was calculated using the Mann-Whitney *U* test for unpaired data (GraphPad Prism version 4.0; GraphPad Software). Differences were considered significant when $P < 0.05$.

Online supplemental material. Fig. S1 shows time kinetics of T cell division occurring in the DLN, nondraining LN, and spleen after an i.p. OVA injection. Fig S2 shows the T cell response after an i.m. injection with OVA or OVA-alum (A), and the Ag uptake by DCs and inflammatory monocytes in the muscle or DLN (B and C). Fig. S3 shows the Gr-1$^+$IL-4$^+$ cell populations 24 h after injection of OVA or OVA-alum in spleens of 4-Get mice. Fig. S4 shows the percentage of CD11c$^+$ cells 24 h after either an i.p. or i.t. injection of DT in CD11c-DTR Tg mice. The online version of this article is available at http://www.jem.org/cgi/content/full/jem.20071097/DC1.

The authors would like to thank Jurg Tschopp and Thibault Desmedt for helpful discussions.

Mirjam Kool is supported by a grant of the Dutch Asthma Foundation, and Hamida Hammad and Bart N. Lambrecht are supported by grants of the Dutch Organisation for Scientific Research VENI and VIDI grants. Bart N. Lambrecht is a recipient of the European Respiratory Society "Romain Pauwels" grant and of an Odysseus grant of the Flemish Government.

The authors have no conflicting financial interests.

Submitted: 30 May 2007
Accepted: 28 February 2008

REFERENCES

1. Naim, J.O., C.J. van Oss, W. Wu, R.F. Giese, and P.A. Nickerson. 1997. Mechanisms of adjuvancy: I–Metal oxides as adjuvants. *Vaccine*. 15:1183–1193.
2. Brewer, J.M., M. Conacher, C.A. Hunter, M. Mohrs, F. Brombacher, and J. Alexander. 1999. Aluminium hydroxide adjuvant initiates strong antigen-specific Th2 responses in the absence of IL-4- or IL-13-mediated signaling. *J. Immunol.* 163:6448–6454.
3. Brewer, J.M., M. Conacher, M. Gaffney, M. Douglas, H. Bluethmann, and J. Alexander. 1998. Neither interleukin-6 nor signalling via tumour necrosis factor receptor-1 contribute to the adjuvant activity of Alum and Freund's adjuvant. *Immunology*. 93:41–48.

4. Brewer, J.M., M. Conacher, A. Satoskar, H. Bluethmann, and J. Alexander. 1996. In interleukin-4-deficient mice, alum not only generates T helper 1 responses equivalent to Freund's complete adjuvant, but continues to induce T helper 2 cytokine production. *Eur. J. Immunol.* 26:2062–2066.
5. Jordan, M.B., D.M. Mills, J. Kappler, P. Marrack, and J.C. Cambier. 2004. Promotion of B cell immune responses via an alum-induced myeloid cell population. *Science.* 304:1808–1810.
6. Gavin, A.L., K. Hoebe, B. Duong, T. Ota, C. Martin, B. Beutler, and D. Nemazee. 2006. Adjuvant-enhanced antibody responses in the absence of toll-like receptor signalling. *Science.* 314:1936–1938.
7. Brewer, J.M. 2006. (How) do aluminium adjuvants work? *Immunol. Lett.* 102:10–15.
8. Mannhalter, J.W., H.O. Neychev, G.J. Zlabinger, R. Ahmad, and M.M. Eibl. 1985. Modulation of the human immune response by the non-toxic and non-pyrogenic adjuvant aluminium hydroxide: effect on antigen uptake and antigen presentation. *Clin. Exp. Immunol.* 61:143–151.
9. Wijburg, O.L., G.P. van den Dobbelsteen, J. Vadolas, A. Sanders, R.A. Strugnell, and N. van Rooijen. 1998. The role of macrophages in the induction and regulation of immunity elicited by exogenous antigens. *Eur. J. Immunol.* 28:479–487.
10. Bomford, R. 1980. The comparative selectivity of adjuvants for humoral and cell-mediated immunity. *Clin. Exp. Immunol.* 39:435–441.
11. Grun, J.L., and P.H. Maurer. 1989. Different T helper cell subsets elicited in mice utilizing two different adjuvant vehicles: the role of endogenous interleukin 1 in proliferative responses. *Cell. Immunol.* 121:134–145.
12. Banchereau, J., and R.M. Steinman. 1998. Dendritic cells and the control of immunity. *Nature.* 392:245–252.
13. Shi, Y., J.E. Evans, and K.L. Rock. 2003. Molecular identification of a danger signal that alerts the immune system to dying cells. *Nature.* 425:516–521.
14. Idzko, M., H. Hammad, M. van Nimwegen, M. Kool, M.A. Willart, F. Muskens, H.C. Hoogsteden, W. Luttmann, D. Ferrari, F. Di Virgilio, et al. 2007. Extracellular ATP triggers and maintains asthmatic airway inflammation by activating dendritic cells. *Nat. Med.* 13:913–919.
15. Bendelac, A., and R. Medzhitov. 2002. Adjuvants of immunity: harnessing innate immunity to promote adaptive immunity. *J. Exp. Med.* 195:F19–F23.
16. De Smedt, T., B. Pajak, E. Muraille, L. Lespagnard, E. Heinen, P. DeBaetselier, J. Urbain, O. Leo, and M. Moser. 1996. Regulation of dendritic cell numbers and maturation by lipopolysaccharide in vivo. *J. Exp. Med.* 184:1413–1424.
17. De Becker, G., V. Moulin, B. Pajak, C. Bruck, M. Francotte, C. Thiriart, J. Urbain, and M. Moser. 2000. The adjuvant monophosphoryl lipid A increases the function of antigen- presenting cells. *Int. Immunol.* 12:807–815.
18. Shah, J.A., P.A. Darrah, D.R. Ambrozak, T.N. Turon, S. Mendez, J. Kirman, C.Y. Wu, N. Glaichenhaus, and R.A. Seder. 2003. Dendritic cells are responsible for the capacity of CpG oligodeoxynucleotides to act as an adjuvant for protective vaccine immunity against Leishmania major in mice. *J. Exp. Med.* 198:281–291.
19. Fujii, S., K. Shimizu, C. Smith, L. Bonifaz, and R.M. Steinman. 2003. Activation of natural killer T cells by α-galactosylceramide rapidly induces the full maturation of dendritic cells in vivo and thereby acts as an adjuvant for combined CD4 and CD8 T cell immunity to a coadministered protein antigen. *J. Exp. Med.* 198:267–279.
20. Sun, H., K.G. Pollock, and J.M. Brewer. 2003. Analysis of the role of vaccine adjuvants in modulating dendritic cell activation and antigen presentation in vitro. *Vaccine.* 21:849–855.
21. Li, H., S. Nookala, and F. Re. 2007. Aluminum hydroxide adjuvants activate caspase-1 and induce IL1-b and IL-18 release. *J. Immunol.* 178:5271–5276.
22. Schnare, M., G.M. Barton, A.C. Holt, K. Takeda, S. Akira, and R. Medzhitov. 2001. Toll-like receptors control activation of adaptive immune responses. *Nat. Immunol.* 2:947–950.
23. Lambrecht, B.N., R.A. Pauwels, and B. Fazekas De St Groth. 2000. Induction of rapid T cell activation, division, and recirculation by intratracheal injection of dendritic cells in a TCR transgenic model. *J. Immunol.* 164:2937–2946.
24. Shiow, L.R., D.B. Rosen, N. Brdickova, Y. Xu, J. An, L.L. Lanier, J.G. Cyster, and M. Matloubian. 2006. CD69 acts downstream of interferon-alpha/beta to inhibit S1P1 and lymphocyte egress from lymphoid organs. *Nature.* 440:540–544.
25. Johansson-Lindbom, B., M. Svensson, M.A. Wurbel, B. Malissen, G. Marquez, and W. Agace. 2003. Selective generation of gut tropic T cells in gut-associated lymphoid tissue (GALT): requirement for GALT dendritic cells and adjuvant. *J. Exp. Med.* 198:963–969.
26. Randolph, G.J., K. Inaba, D.F. Robbiani, R.M. Steinman, and W.A. Muller. 1999. Differentiation of phagocytic monocytes into lymph node dendritic cells in vivo. *Immunity.* 11:753–761.
27. Geissmann, F., S. Jung, and D.R. Littman. 2003. Blood monocytes consist of two principal subsets wih distinct migratory properties. *Immunity.* 19:71–82.
28. Voehringer, D., K. Shinkai, and R.M. Locksley. 2004. Type 2 immunity reflects orchestrated recruitment of cells committed to IL-4 production. *Immunity.* 20:267–277.
29. Sixt, M., N. Kanazawa, M. Selg, T. Samson, G. Roos, D.P. Reinhardt, R. Pabst, M.B. Lutz, and L. Sorokin. 2005. The conduit system transports soluble antigens from the afferent lymph to resident dendritic cells in the T cell area of the lymph node. *Immunity.* 22:19–29.
30. Pape, K.A., D.M. Catron, A.A. Itano, and M.K. Jenkins. 2007. The Humoral Immune Response Is Initiated in Lymph Nodes by B Cells that Acquire Soluble Antigen Directly in the Follicles. *Immunity.* 26:491–502.
31. Jung, S., D. Unutmaz, P. Wong, G. Sano, K. De los Santos, T. Sparwasser, S. Wu, S. Vuthoori, K. Ko, F. Zavala, et al. 2002. In vivo depletion of CD11c(+) dendritic cells abrogates priming of CD8(+) T cells by exogenous cell-associated antigens. *Immunity.* 17:211–220.
32. van Rijt, L.S., S. Jung, A. Kleinjan, N. Vos, M. Willart, C. Duez, H.C. Hoogsteden, and B.N. Lambrecht. 2005. In vivo depletion of lung $CD11c^+$ dendritic cells during allergen challenge abrogates the characteristic features of asthma. *J. Exp. Med.* 201:981–991.
33. Chen, C.J., Y. Shi, A. Hearn, K.A. Fitzgerald, D. Golenbock, G. Reed, S. Akira, and K.L. Rock. 2006. MyD88-dependent IL-1 receptor signaling is essential for gouty inflammation stimulated by monosodium urate crystals. *J. Clin. Invest.* 116:2262–2271.
34. Martinon, F., V. Petrilli, A. Mayor, A. Tardivel, and J. Tschopp. 2006. Gout-associated uric acid crystals activate the NALP3 inflammasome. *Nature.* 440:237–241.
35. Tilney, N.L. 1971. Patterns of lymphatic drainage in the adult laboratory rat. *J. Anat.* 109:369–383.
36. Abernethy, N.J., W. Chin, J.B. Hay, H. Rodela, D. Oreopoulos, and M.G. Johnston. 1991. Lymphatic drainage of the peritoneal cavity in sheep. *Am. J. Physiol.* 260:F353–F358.
37. Itano, A.A., S.J. McSorley, R.L. Reinhardt, B.D. Ehst, E. Ingulli, A.Y. Rudensky, and M.K. Jenkins. 2003. Distinct dendritic cell populations sequentially present antigen to CD4 T cells and stimulate different aspects of cell-mediated immunity. *Immunity.* 19:47–57.
38. van Vugt, E., E.W. Kamperdijk, and R.H. Beelen. 1993. Migration patterns of rat peritoneal macrophages and dendritic cells. *Transplant. Proc.* 25:2808–2810.
39. Steinman, R.M., D. Hawiger, and M.C. Nussenzweig. 2003. Tolerogenic dendritic cells. *Annu. Rev. Immunol.* 21:685–711.
40. Brimnes, M.K., L. Bonifaz, R.M. Steinman, and T.M. Moran. 2003. Influenza virus–induced dendritic cell maturation is associated with the induction of strong T cell immunity to a coadministered, normally nonimmunogenic protein. *J. Exp. Med.* 198:133–144.
41. Fujii, S., K. Liu, C. Smith, A.J. Bonito, and R.M. Steinman. 2004. The linkage of innate to adaptive immunity via maturing dendritic cells in vivo requires CD40 ligation in addition to antigen presentation and CD80/86 costimulation. *J. Exp. Med.* 199:1607–1618.
42. Serbina, N.V., T.P. Salazar-Mather, C.A. Biron, W.A. Kuziel, and E.G. Pamer. 2003. TNF/iNOS-producing dendritic cells mediate innate immune defense against bacterial infection. *Immunity.* 19:59–70.
43. Tacke, F., F. Ginhoux, C. Jakubzick, N. van Rooijen, M. Merad, and G.J. Randolph. 2006. Immature monocytes acquire antigens from other

cells in the bone marrow and present them to T cells after maturing in the periphery. *J. Exp. Med.* 203:583–597.
44. Naik, S.H., D. Metcalf, A. van Nieuwenhuijze, I. Wicks, L. Wu, M. O'Keeffe, and K. Shortman. 2006. Intrasplenic steady-state dendritic cell precursors that are distinct from monocytes. *Nat. Immunol.* 7:663–671.
45. Pasare, C., and R. Medzhitov. 2005. Control of B-cell responses by Toll-like receptors. *Nature.* 438:364–368.
46. Schmitz, N., M. Kurrer, and M. Kopf. 2003. The IL-1 receptor 1 is critical for Th2 cell type airway immune responses in a mild but not in a more severe asthma model. *Eur. J. Immunol.* 33:991–1000.
47. Tramontini, N., C. Huber, R. Liu-Bryan, R.A. Terkeltaub, and K.S. Kilgore. 2004. Central role of complement membrane attack complex in monosodium urate crystal-induced neutrophilic rabbit knee synovitis. *Arthritis Rheum.* 50:2633–2639.
48. van Gisbergen, K.P., T.B. Geijtenbeek, and Y. van Kooyk. 2005. Close encounters of neutrophils and DCs. *Trends Immunol.* 26:626–631.
49. De Heer, H.J., H. Hammad, T. Soullie, D. Hijdra, N. Vos, M.A. Willart, H.C. Hoogsteden, and B.N. Lambrecht. 2004. Essential role of lung plasmacytoid dendritic cells in preventing asthmatic reactions to harmless inhaled antigen. *J. Exp. Med.* 200:89–98.